Using ForeStereo and LIDAR data to assess fire and canopy structure-related risks in relict *Abies pinsapo* Boiss. forests

Álvaro Cortés-Molino[1], Isabel Aulló-Maestro[2,3],
Ismael Fernandez-Luque[1], Antonio Flores-Moya[1], José A. Carreira[4] and
A. Enrique Salvo[1]

[1] Departamento de Botánica y Fisiología Vegetal, Universidad de Málaga, Málaga, Spain
[2] Escuela Técnica Superior de Ingeniería de Montes, Forestal y del Medio Natural, Universidad Politécnica de Madrid, Madrid, Spain
[3] Departamento de Silvicultura y Gestión Forestal, Instituto Nacional de Investigación y Tecnología Agraria y Alimentaria, Centro de Investigación Forestal (INIA-CIFOR), Madrid, Spain
[4] Departamento de Biología Animal, Biología Vegetal y Ecología, Universidad de Jaén, Jaén, Spain

ABSTRACT

In this study we combine information from aerial LIDAR and hemispherical images taken in the field with ForeStereo—a forest inventory device—to assess the vulnerability and to design conservation strategies for endangered Mediterranean fir forests based on the mapping of fire risk and canopy structure spatial variability. We focused on the largest continuous remnant population of the endangered tree species *Abies pinsapo* Boiss. spanning 252 ha in Sierra de las Nieves National Park (South Andalusia, Spain). We established 49 sampling plots over the study area. Stand structure variables were derived from ForeStereo device, a proximal sensing technology for tree diameter, height and crown dimensions and stand crown cover and basal area retrieval from stereoscopic hemispherical images photogrammetry. With this information, we developed regression models with airborne LIDAR data (spatial resolution of 0.5 points·m^{-2}). Thereafter, six fuel models were fitted to the plots according to the UCO40 classification criteria, and then the entire area was classified using the Nearest Neighbor algorithm on Sentinel imagery (overall accuracy of 0.56 and a KIA-Kappa Coefficient of 0.46). FlamMap software was used for fire simulation scenarios based on fuel models, stand structure, and terrain data. Besides the fire simulation, we analyzed canopy structure to assess the status and vulnerability of this fir population. The assessment shows a secondary growth forest that has an increasing presence of fuel models with the potential for high fire spread rate fire and burn probability. Our methodological approach has the potential to be integrated as a support tool for the adaptive management and conservation of *A. pinsapo* across its whole distribution area (<4,000 ha), as well as for other endangered circum-Mediterranean fir forests, as *A. numidica* de Lannoy and *A. pinsapo marocana* Trab. in North Africa.

Subjects Ecosystem Science, Climate Change Biology, Natural Resource Management, Environmental Impacts, Forestry
Keywords Fir forests, Hemispherical images, Remote sensing, Forest conservation, Airborne LIDAR, Fire simulations

INTRODUCTION

Endemic conifer species are more numerous in Mediterranean-type climate regions in the Northern Hemisphere than in the Southern Hemisphere, which has been linked to the selective pressure of cold and/or drought conditions that led to the development of ecophysiological advantages for conifers over angiosperms on oligotrophic soils. Meanwhile, the Mediterranean-type climate regions of South Africa and Southwestern Australia have been more climatically and tectonically stable, which resulted in lower diversity and persistence of ancient lineages of conifers. The Mediterranean Basin has 32 endemic conifer species, accounting for more than 25% of the total conifer flora of 122 species (*Rundel, 2019*). In particular, the genus *Abies* Mill. experienced extensive speciation from the late Neogene that gave rise to nine species and one natural hybrid in the Mediterranean Basin (*Linares, 2011*). Past climate changes have led to population migrations, and to shrinkage and fragmentation of ancestral Mediterranean fir populations, further exacerbated by human impacts. This resulted in circum-Mediterranean endemic firs of high paleogeographic interest, since they are established in relict restricted-range populations with relevant vulnerability to global warming effects (*Liepelt et al., 2010*). Adaptive management of these forests to protect them from the increasing fire risk is essential for their survival.

Extreme climate events, such as severe droughts, mega-fires, and disease infestations threaten these relict Mediterranean fir populations (*Sánchez-Salguero et al., 2017*). It is well known that fire has influenced the landscape and terrestrial life as far back as the beginning of land plants (*Bowman et al., 2009*; *Pausas & Keeley, 2009*; *He et al., 2012*). Although many conifers have developed adaptive traits to live in fire-prone environments, this is not the case for the genus *Abies*. The firs developed traits appropriate for the humid areas where they thrive, which has rendered them neither resistant (thin bark) nor resilient (recruitment failure in open spaces) to fires (*Furyaev, Wein & MacLean, 1983*; *Vega Hidalgo, 1999*).

Remote sensing is useful for assessment and development of measures for mitigation of the effects of global warming in relict Mediterranean fir forests. Spectral imagery has been employed for the early detection of forest pathogen infestations (*Immitzer & Atzberger, 2014*), to estimate evapotranspiration (*Dzikiti et al., 2019*), and to study photosynthetic activity (*De Sousa et al., 2017*). Meanwhile, 3D point cloud data from laser scanning (LIDAR) have been employed in fire management (*Chuvieco & Kasischke, 2007*) and to assess forest volume, biomass (*Van Ardt, Wynne & Scrivani, 2008*), and canopy structure (*Adamic et al., 2017*; *Mura et al., 2015*). Also, the point cloud can be used for ecological purposes, such as assessing light availability for species distribution modeling (*Wüest et al., 2020*) and forest changes in ecotones (*Wang, Ginzler & Waser, 2020*). Airborne LIDAR has shown better suitability for mapping crown and canopy heights (*Wang & Glenn, 2008*), although in high density forests the point cloud may not reach the ground, and thus mapping understory vegetation may be inaccurate. However, terrestrial LIDAR has a great potential for estimating shrub and understory biomass,

although there are insufficient points for a precise estimation of crown heights when the canopy cover is high (*Hilker et al., 2012*).

Mapping fire risk with the support of remote sensing tools is becoming essential for landscape planning in the Mediterranean Basin. High-precision fuel moisture and flammability spatial modeling is achieved by combining satellite and meteorological data into radiative transfer models (*Chuvieco et al., 2006*; *Yebra et al., 2018*). Burn probability is then assessed through algorithms such as the Minimum Travel Time (MTT) based on the Huygens' principle (*Finney, 2002*). Several studies have previously applied MTT through FlamMap software on fuel spatial models to assess fire risk in Mediterranean-type ecosystems of Greece (*Mitsopoulos, Mallinis & Arianoutsu, 2015*; *Mallinis et al., 2016*), Italy (*Salis et al., 2015*) and Spain (*Molina, Rodríguez y Silva & Herrera, 2017*; *Alcasena et al., 2019*). In this last study, fire risk and highly vulnerable areas were mapped for the whole Catalonia region by applying the *Scott & Burgan (2005)* fuel model classification on vegetation structure data and running MTT through FlamMap to obtain 150 m resolution fire scenarios. Alternatively, fire spread from specific ignition events can be forecasted, for example, *Salis et al. (2016)* used the FARSITE software to derive fire spread simulations for several Euro-Mediterranean countries along an east-west gradient. All these studies agree that accurate and customized fuel models are key for assessing burn probability and fire risk.

In this respect, airborne LIDAR technology provides an unprecedented tool for fuel and canopy structure characterization in forest ecosystems. However, several studies highlighted limitations of this technology for accurate understory fuel mapping due to the lack of points reaching the ground (*González-Olabarria et al., 2012*; *Botequim et al., 2019*). Therefore, LIDAR data need to be implemented in regression models supported by field sampling to eventually characterize the forest structure. For this purpose, hemispherical images are an alternative to traditional field sampling. This technique has been used in forest ecology for more than 50 years, but its widespread adoption was limited due to constraints related to image processing capacity (*Chianucci, 2019*). However, technical improvements allowed reducing the time for image processing as well as better image quality acquisition. The widespread proliferation of digital cameras has increased the ease of obtaining and storing hemispherical images, which have become an important tool for fieldwork (*Hall, Fournier & Rich, 2017*). ForeStereo, a forest inventorying device patented by the Forest Research Centre of the Spanish National Institute for Agriculture and Food Research and Technology (CIFOR-INIA), allows one to obtain stand and tree variables in a cost-effective way by processing pairs of stereoscopic hemispherical images taken at a sampling location (*Rodríguez-García et al., 2014*).

Most studies applying LIDAR to circum-Mediterranean fir forests have focused on the most widely distributed *Abies alba* Mill., whereas those focusing on other species such as the relicts *A. pinsapo* Boiss. and *A. numidica* de Lannoy, which are becoming increasingly vulnerable to global change impacts (*Liepelt et al., 2010*), are very scant. *Aragón, Navarro Cerrillo & Mesas Carrascosa (2019)* and *Cortés-Molino et al. (2017)* studied *A. pinsapo* Boiss. forests using LIDAR, but only for basic tree identification and vegetation landscape analysis, respectively. Now, the combination of remote sensing

technology such as laser scanning and proximal sensing (e.g., ForeStereo) can contribute to the monitoring of these relict forests through the acquisition of high-precision stand structure data.

Abies pinsapo is restricted to a few areas in the southern Iberian Peninsula (*A. pinsapo pinsapo*) and northern Morocco (*Abies pinsapo marocana*), totaling less than 8,000 ha (*Linares, 2008*). Forest fires have markedly reduced the size of populations of this fir; in some localities the longest timespan without fires in the period 1817–1997 was just 34 years (*Vega Hidalgo, 1999*). Thus, fire is considered the most important threat for the conservation and survival of this endangered species (*López-Quintanilla et al., 2013*). *A. pinsapo* shows a very low resistance to fire due to its thin bark, despite its relatively low fuel flammability and low fire spread rates in dense stands, due to sparse understory and relatively humid conditions (*Rodríguez y Silva, 1996*). Additionally, acute symptoms of tree growth decline and forest dieback due to stand stagnation and climate change have already been reported in some populations (*Linares & Carreira, 2009*), where *Pinus halepensis* Mill. is increasing in abundance, turning previously pure *A. pinsapo* stands into mixed ones (*Linares, Delgado-Huertas & Carreira, 2011*).

Our work aimed to combine the use of LIDAR and hemispherical images to study one of the most significant *A. pinsapo* populations, located in a protected area in Málaga (Spain), to assess vulnerability through (i) mapping fire risk and (ii) analyzing canopy structure variability and its possible links to reported declining growth symptoms.
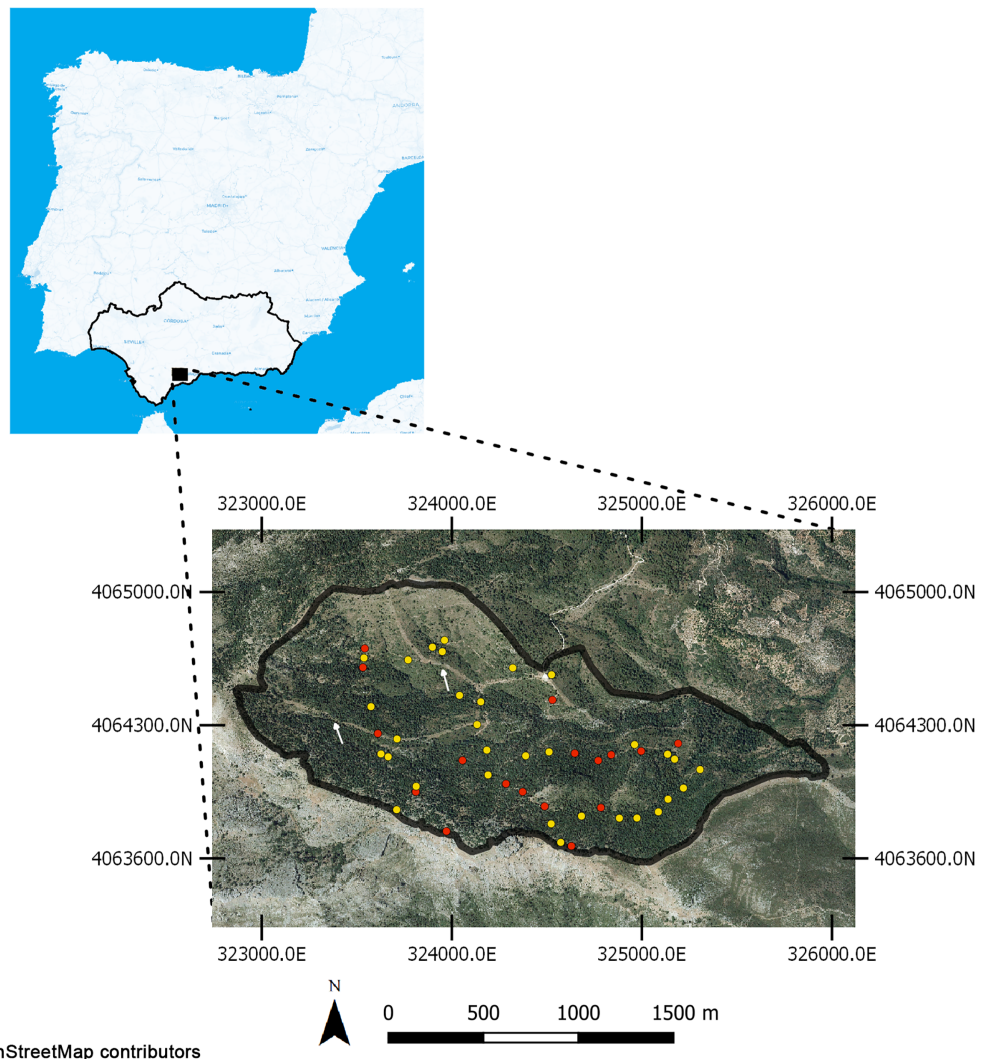
MATERIALS AND METHODS

Study area

The study location is a steep valley of about 250 ha in area in the municipality of Yunquera, in Sierra de las Nieves National Park (Fig. 1), in a transition between the upper and lower Mesomediterranean bioclimatic band. The annual rainfall is around 1,500 mm and the average daily maximum temperature of the warmest month (August) is 33.6 °C (*Rivas-Martínez & Rivas-Sáenz, 1996*). At the southern border of the valley there is a crest that was the limit of a severe wildfire in 1991 that burned 9,000 ha (*Narváez, 1991*). The eastern part is bordered by crop fields. This, together with summer weather conditions and significant touristic pressure in Sierra de las Nieves National Park, makes the risk of wildfire especially high. This forest belongs to the *Paeonio broteroi-Abietetum pinsapo* (*Asensi & Rivas-Martínez, 1976*) vegetation association composed mainly of pinsapo fir, forming single-species stands in the upper and shaded parts of the valley. The incidence of the root-rot fungus *Heterobasidion abietinum* Niemelä & Korhonen is very high (*Linares et al., 2010*). In sunny and low-altitude spots, the forest includes *Pinus halepensis* and shrubs of *Juniperus* spp and *Cistus* spp.

Fieldwork: ForeStereo inventory

The purpose of the fieldwork was to classify local fuel models and collect forest structure data, mainly canopy cover, and crown and stand heights. The valley was sampled in Spring 2018 with 49 plots of 8 m radius (201.06 m^2), using stereoscopic hemispherical images

Figure 1 Study area location, in the National Park of Sierra de las Nieves (Andalusia, Spain). Forty-nine plots were used in the field-based sampling for calibration purposes using ForeStereo device. Yellow points are training plots, red ones are validation plots. White arrows indicate the firewalls opened on the area. Base map and data from OpenStreetMap and OpenStreetMap Foundation.

Full-size ☒ DOI: 10.7717/peerj.10158/fig-1

for obtaining tree metrics such as stand height (Ho), Canopy Base Height (CBH), Canopy Cover (CC), Canopy Bulk Density (CBD) and basal area (G). Shrub cover and height were also assessed by the line-intersect method to support the classification of the fuel models. Each sampling plot was accurately geolocated using a high precision GNSS receiver, supported by an RTK terrestrial station deployed in the upper part of the valley. We assumed a maximum error of 1 m in each plot, due to the difficulty of getting GNSS coverage in high dense canopy.

Access to field sites was approved by the Andalusian Regional Government (Consejería de Medio Ambiente y Ordenación del Territorio) with the approval code: *PNSN/AU/10-2018*.
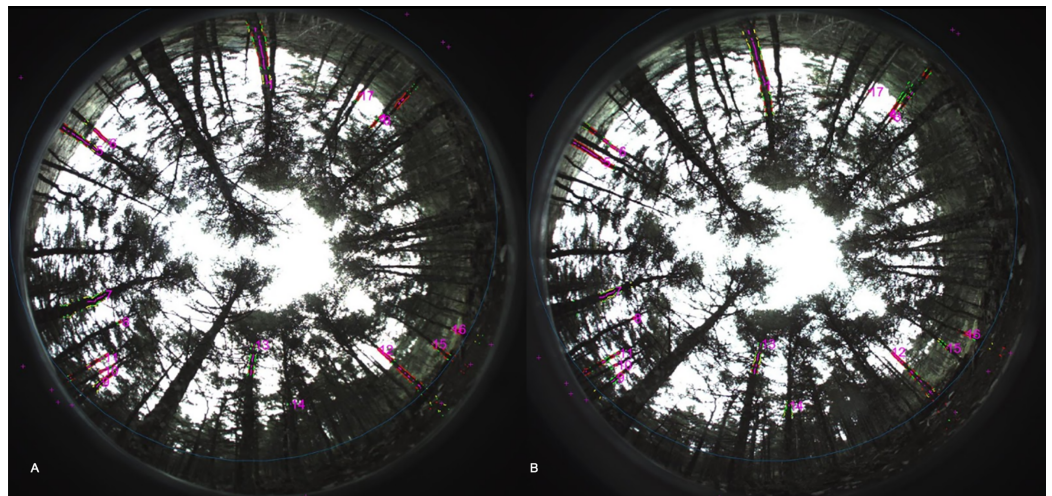
Figure 2 Example of hemispherical pair images obtained with ForeStereo to characterize forest stand canopy structure at the field sampling plots. (A) and (B) are both stereoscopic images obtained at the same time in each plot. Full-size 🖼 DOI: 10.7717/peerj.10158/fig-2

Forest inventory was derived using ForeStereo, a device developed by the Forest Research Centre of the Spanish National Institute for Agriculture and Food Research and Technology (INIA-CIFOR). ForeStereo is equipped with two upward-looking fish-eye cameras. At each sampling location three pairs of hemispherical stereoscopic images (Fig. 2) with different exposures are taken. The matching process, compiled in a MatLab® software package, consists of four main steps as detailed in *Sánchez-González et al. (2016)*: (i) a supervised segmentation of tree stems and crowns; (ii) correspondence of features between the two images and photogrammetric retrieval of tree dimensions; (iii) tree variable modeling and (iv) stand variable estimation, which requires correction of instrumental bias and occlusions (*Montes et al., 2019*). ForeStereo was used to estimate tree height, crown base height, crown volume and diameter at breast height (DBH) for each tree, number of stems per hectare and crown cover (CC) and stand basal area (G). Tree metrics from the hemispherical images were compared with airborne LIDAR output data to develop regression models. Thirty-two of the plots were randomly chosen to adjust the models, and the remaining seventeen plots were used to assess the models' predictive capability.

Because the geometry of the ForeStereo system and image projections is known, no additional data calibration is needed to carry out photogrammetric retrieval of tree variables. Accuracy of ForeStereo estimated through the Root Mean Squared Error (RMSE) ranges from 0.015 to 0.057 m for DBH (*Rodríguez-García et al., 2014*; *Sánchez-González et al., 2016*), 2.59 to 6.4 m for tree height (*Rodríguez-García et al., 2014*; *Marino et al., 2018*) and 3.1 and 0.6 m for crown base height and crown diameter respectively (*Marino et al., 2018*), and 11.6 m^2/ha for G (*Sánchez-González et al., 2016*).

With the ForeStereo data we were able to estimate stand height at each plot following the Assmann's criteria (*Assman, 1970*), whereas the canopy cover was obtained directly from the hemispherical images, and the Canopy Base Height (CBH) was averaged for each

plot. The calculation of the Canopy Bulk Density (CBD) was based on equations reported by *Ruiz-Peinado, Del Río & Montero (2011)* for *A. pinsapo*, in which tree height and stem diameter are used to calculate thin branch and needle biomass. Therefore, CBD is estimated by dividing biomass by crown volume (which is obtained from ForeStereo estimates).

LIDAR data

The LIDAR data were obtained in 2015 by the Spanish National Geographic Institute, through the "Plan Nacional de Ortofotografía Aérea (PNOA)" project. The point cloud density is 0.5 points·m^{-2}. FUSION software was employed for point cloud processing and data extraction (*McGaughey & Carson, 2003*). A correlation matrix between ForeStereo tree data and all LIDAR metrics obtained with FUSION was useful to detect which LIDAR metric was most suitable to build the regression models in 32 random plots. We selected the best correlation results ($R < 0.5$, p-value < 0.05) to test linear, power and exponential regression models. The models with less root-mean-square error (RMSE) and higher adjusted-R in the remaining 17 plots were chosen to predict ForeStereo tree metrics from the LIDAR point cloud. Height break for LIDAR metrics was 4 m, whereas it was 0.25 m for the total vegetation height to avoid high shrubs influence and ground points, respectively. These two height breaks were tested to inquire which one was the better to fit the models.

General canopy structure traits such as canopy cover and height were analyzed from the regression models obtained to detect symptoms of declining growth in this *A. pinsapo* forest. These variables were chosen because airborne LIDAR can estimate them accurately (*Ahmed et al., 2015*; *Arumäe & Lang, 2018*). Also, we tested whether canopy bulk density was consistent with the results from this analysis.

Fuel models and fire scenarios

To simulate fire risk, we first classified field plots according to the UCO40 fuel models, which use specific criteria and traits appropriate for Mediterranean environments and thus perform better than the widely used Prometheus or Rothermel models (*Rodríguez y Silva & Molina Martínez, 2010*, *2012*). We identified a total of six fuel models across the plots (Table 1; Fig. 3). The UCO4 procedure is based on the fuel models classification of *Scott & Burgan (2005)*, but adapted for southern Iberian Peninsula climate conditions through providing hybrid model types that represent fuel traits and their evolution. Shrub and climate characteristics have shown different behaviors between American and Mediterranean fuel models, so parameters such as fuel load and fuelbed depth must be adjusted (*Rodríguez y Silva & Molina-Martínez, 2012*).

Ecognition® software was used to segment the place of study using the Nearest Neighbor algorithm in an Object-Based Image Analysis (OBIA) (*Gao et al., 2007*). To carry out this segmentation, we used the raster layers resulting from the regression models validated previously (CBD, CBH, G, Ho) along with NDVI data from Sentinel-2 images (2015) and terrain models obtained from the LIDAR point cloud (topography, aspect, and

Table 1 Fuel model classification obtained following the UCO40 criteria (*Rodríguez y Silva & Molina-Martínez, 2012*), based on *Scott & Burgan (2005)*. Dead fuel models are classified by the time lag: the time required for the moisture content of a fuel to respond to within 2/3 of the new equilibrium moisture content. Larger diameter fuels have longer time lags, so they respond slower to environmental changes (*Anderson, 1982*). LiveH: Live herbaceous fuel, LiveW: Live wood fuel. Moisture of extinction (%): moisture content that prevents flame from propagating.

Fuel type	Fuel loading (tn/ha)					Moisture of extinction (%)	Fuel bed depth (cm)
	Time lag			LiveH	LiveW		
	1 h	10 h	100 h				
Predominance of shrubs							
M3	11.47	2.88	3.37	0	6.10	15	82.29
M8	11.23	6.10	3.47	0	7.27	30	121.92
M9	34.71	9.86	4.93	0	18.89	15	182.88
Pine-needle litter with shrubs and/or grassland under forest canopy							
HPM4	17.63	13.23	1.17	0	11.13	20	76.2
Predominance of pine-needle with branches and other canopy debris							
HR7	0.73	3.76	3.47	0	0	25	18.28
Predominance of canopy debris accumulation							
R4	1.57	5.16	6.29	0	0	25	82

slope). Later, a confusion matrix was calculated to evaluate the accuracy of the fuel model classification.

The following raster layers generated from the regression models were incorporated: terrain elevation, aspect, slope, Ho, CBH, CBD, CC, and fuel models.

The initial fuel moisture file (.FMD) used was based on *Scott & Burgan (2005)* suggestions. We assumed a low moisture content (two-third cured) for the fuel more commonly found in north-facing slopes (fuel models M8, HR7 and R4; see Table 1) and very low moisture content (fully cured) for the fuel models more frequently found in south-facing slopes (M3, M9 and HPM4). A Weather Stream file (.WXS) with typical values of circadian change under summer weather conditions in the area was used for dead fuel moisture conditioning (Table 2). This file modifies initial dead fuel moisture based on changes during a given period in weather variables such as temperature, relative humidity, cloud cover and hourly precipitation. Conditioning also implies adjusting initial dead fuel moisture to site factors (elevation, slope, aspect, and canopy cover), based on the corresponding raster layers previously uploaded in FlamMap (*Finney, 2006*). The .WXS file was built from meteorological data that are continuously recorded in situ by the University of Jaén (values of temperature, precipitation and relative humidity) and from records of the Spanish Meteorological Agency-AEMET (values of wind and cloud cover). We chose the warmest day of 2014 (available recorded data) for the conditioning period between the 10:00 and 19:00 h without precipitations or any cloud cover. The conditioned fuel moistures at the end of this period were the final fuel moistures used for the simulations.

Figure 3 Example of the six fuel models identified in the plots based on *Rodríguez y Silva & Molina Martínez's (2010)* handbook. (A) R4 model: Predominance of canopy debris accumulation (B) HR7 model: Predominance of pine needle with branches (C) HPM4 model: Pine-needle with shrubs and grass (D) M3 model: Predominance of shrubs with a fuel bed close to 1 m (E) M8 model: Predominance of shrubs with grass with a fuel bed of 120 m. (F) M9 model: Predominance of thick shrubs with a fuel bed over 175 m.   Full-size ☑ DOI: 10.7717/peerj.10158/fig-3

Table 2 **Dead fuel moisture conditioning.** Weather stream file (.WXS) showing typical summer weather circadian change in the area, used as input to Flammap software for quantifying the moisture of dead fuel.

Date	T (°C)	RH (%)	PP (mm)	Wind SP (m/s)	Wind dir. (°)	Cloud (%)
08/27/14 10:00	28	33	0	2	180	0
08/27/14 11:00	29	32	0	2	180	0
08/27/14 12:00	30	29	0	1	180	0
08/27/14 13:00	31	27	0	2	180	0
08/27/14 14:00	30	27	0	2	180	0
08/27/14 15:00	29	28	0	2	180	0
08/27/14 16:00	29	29	0	2	180	0
08/27/14 17:00	28	30	0	1	180	0
08/27/14 18:00	27	31	0	2	180	0
08/27/14 19:00	26	32	0	2	180	0

We obtained three different datasets as model outputs: (1) Burn probability based on 200 random ignition points using the MTT algorithm, (2) flame length and (3) flame spread rate, calculated for each cell. The purpose of simulating fire scenarios was to detect vulnerable areas and to assess for conservation planning how exposed the pinsapo forest is to this risk. For this reason, we did not simulate specific events or spotfires using Farsite software. Instead, FlamMap software is more appropriate, because it calculates spread rate and flame length for each landscape cell without a temporal component, and uses MTT to simulate 200 random fires to predict the probability of a point to be burned (*Finney, 2006*; *González-Olabarria et al., 2012*). The simulations were set under two prevailing wind conditions: west winds (locally called "Ponent") and east winds (called "Levant"), both for a typical speed of 13 km·h^{-1}.

RESULTS

We found that the LIDAR metrics that best fit the ForeStereo data were (Table 3): Percentage of first returns above 4 m (x), Percentage of all returns above 4 m (y), Percentage of all returns above mean (z) and Percentage of first returns above 0.25 m (d). All the significant regression models were obtained with 95% confidence in the seventeen validation plots. Basal Area (G) was the only variable with an acceptable fit using a height break of 0.25 m. The rest of the variables were better modeled above 4 m. Canopy Cover (CC) had the best fitting model with an RMSE less than 20%, while the greatest error was found in modeling the Canopy Base Height (CBH) with an RMSE of 83.3%. This high difference could be due to low point cloud density (minimum 0.5 points·m^{-2} guaranteed) as well as the fact that airborne LIDAR produces better accuracy for variables related to the top of the canopy (*Hilker et al., 2012*), such as canopy cover or canopy height, than variables under the canopy. Results for dominant height were acceptable (RMSE of 0.55), because finding the top of the crowns with ForeStereo in high-density forests can be difficult.

Table 3 Best regression models between LIDAR data (independent variable) and field-based Forestereo data (dependent variable), used to map spatial distribution of the main forest structure variables.

Dependent variable	Predictive model	R^2	RMSE (%)
CC	x·0.92023	0.84	17.7
Ho	0.1469·y	0.61	55.7
CBH	$x^{0.013839}$	0.43	83.3
CBD	z·0.007893	0.64	59.5
G	$d·9.28·10^{-8}$	0.61	67.3

Note:
To find which LIDAR data best suit to each field data, a correlation matrix was done. The best results ($R > 0.5$ and p-value < 0.05) were tested by using linear, power and exponential regression models. The models with highest R^2 and lower RMSE were selected. CC: canopy cover; Ho: stand height; CBH: canopy base height; CBD: canopy bulk density; G: basal area. x: Percentage of LIDAR first returns above 4 m, y: Percentage of all returns above 4 m, z: Percentage of all returns above mean, d: Percentage of first returns above 0.25 m.

Table 4 Confusion matrix of the Nearest Neighbor classification for the fuel models. User accuracy: how often the class on the map will actually be present on the ground. Producer accuracy: how often are real features on the ground correctly shown on the classified map.

		Predicted classes						
		M3	M8	M9	HPM4	HR7	R4	Sum
Actual classes	Fuel type observed in field							
	M3	2	0	0	1	2	0	5
	M8	0	5	1	0	0	0	6
	M9	3	0	3	0	0	0	6
	HPM4	0	0	0	2	2	1	5
	HR7	0	1	0	0	0	1	2
	R4	0	0	0	0	0	3	3
	Sum	5	6	4	3	4	5	
	Accuracy							
	Producer	0.4	0.83	0.75	0.7	0	0.6	
	User	0.4	0.83	0.5	0.4	0	1	
	Overall accuracy				KIA			
	0.56				0.46			

The error matrix for the fuel model classification using the Nearest Neighbor algorithm shows an overall accuracy of 0.56 and a Kappa Coefficient (KIA) of 0.46 (Table 4). The most frequent fuel model in the study area was M9 (30.5% of land cover), followed by M3 with 27.4% and M8 with 23%. In all the fuel models, shrubs play a predominant role in the fire behavior. The least frequent fuel models were HPM4 (7.19% of land cover; fire behavior mainly controlled by needle litter together with understory shrubs and/or grasses), HR7 (6.12% of land cover; conifer-needles and branches and other canopy debris play a predominant role) and R4 (5.73% of land cover; predominance of canopy debris accumulation in fire behavior).

Once the corresponding layers were created based on the regression models, the fuel model classifications and the terrain elevation data (Fig. 4), fire simulations under two wind conditions were obtained from FlamMap (Fig. 5). The final landscape file keeps the same pixel resolution of the input data (10 m). We found higher burn probabilities and spread rate under Levant wind conditions, but similar flame length scenarios under both Levant and Ponient winds. Burn probability was higher under Levant winds, with a mean value of 0.078, than under Ponent winds, with a mean value of 0.061. Fire spread rate showed a mean value of 41.82 m·min^{-1} under Levant wind conditions, and more than 50% of the landscape showed spread rates ≥50 m·min^{-1}. In contrast, Ponent winds resulted in lower fire spread rates (mean value of 33.34 m·min^{-1}) and a considerably lower fraction of the landscape (36%) was affected by spread rates ≥50 m·min^{-1}. Flame length values were similar for the fire simulations under both wind directions.

Regarding the canopy structure analysis to detect symptoms of forest decline and dieback, the estimated variables CBH and G were not considered due to RMSEs far above 60%. Instead, we use Ho and CC (Fig. 6), as well as CBD, for such assessment. The following results were estimated only in the landscape cells with a vegetation height above 4 m, in order to exclude non-forest patches of shrubs, as well as forest gaps recently opened due to tree mortality (Fig. 7). Canopy heights (Ho) ranged from 4 to 18 m, with a mean value of 9.1 m and a standard deviation (SD) of 3.28. It is remarkable that the mode of canopy heights falls below 5 m in this forest area not affected by fire since the mid-20th century and under long-term, no management policy. On the other hand, canopy height classes between 7 and 12 m showed similar frequencies (high equitability). Lastly, canopy heights higher than 15 m were present, but with rather low frequency.

Canopy cover had a mean value of 64.5% and an SD of 18. We found low frequencies for values between 0% and 30% (<2% of the area) because most areas with low CC corresponded to land covered by shrubs with less than 4 m heights. Almost 25% of the land showed CC values above 80%, which means that areas with near to full cover are relatively common. Also, 66% of the area had a CC of 40–80%. Lastly, CBD mean value was 0.16 kg·m^{-3} with a SD of 0.1. Our results showed a high canopy density because >60% of the area had values over 0.1 kg·m^{-3} and >30% was over 0.3 kg·m^{-3}.

DISCUSSION

Endangered circum-Mediterranean firs are highly vulnerable to climate change effects in the isolated areas where they remain (*Sánchez-Salguero et al., 2017*). *Abies nebrodensis* Mattei is currently the rarest conifer in the European flora, with only 34 mature trees able to reproduce sexually in the wild (*Pasta et al., 2019*). The recovery of this species and the protection of the other ones to avoid a similar decrease is an urgent matter that demands the best techniques available to support the traditional field survey.

We propose a methodology that combines the use of LIDAR with ForeStereo, UCO40 fuel models, and FlamMap simulations to significantly reduce the effort and time required for fieldwork, increasing the efficiency of the massive data capture required in forest management.
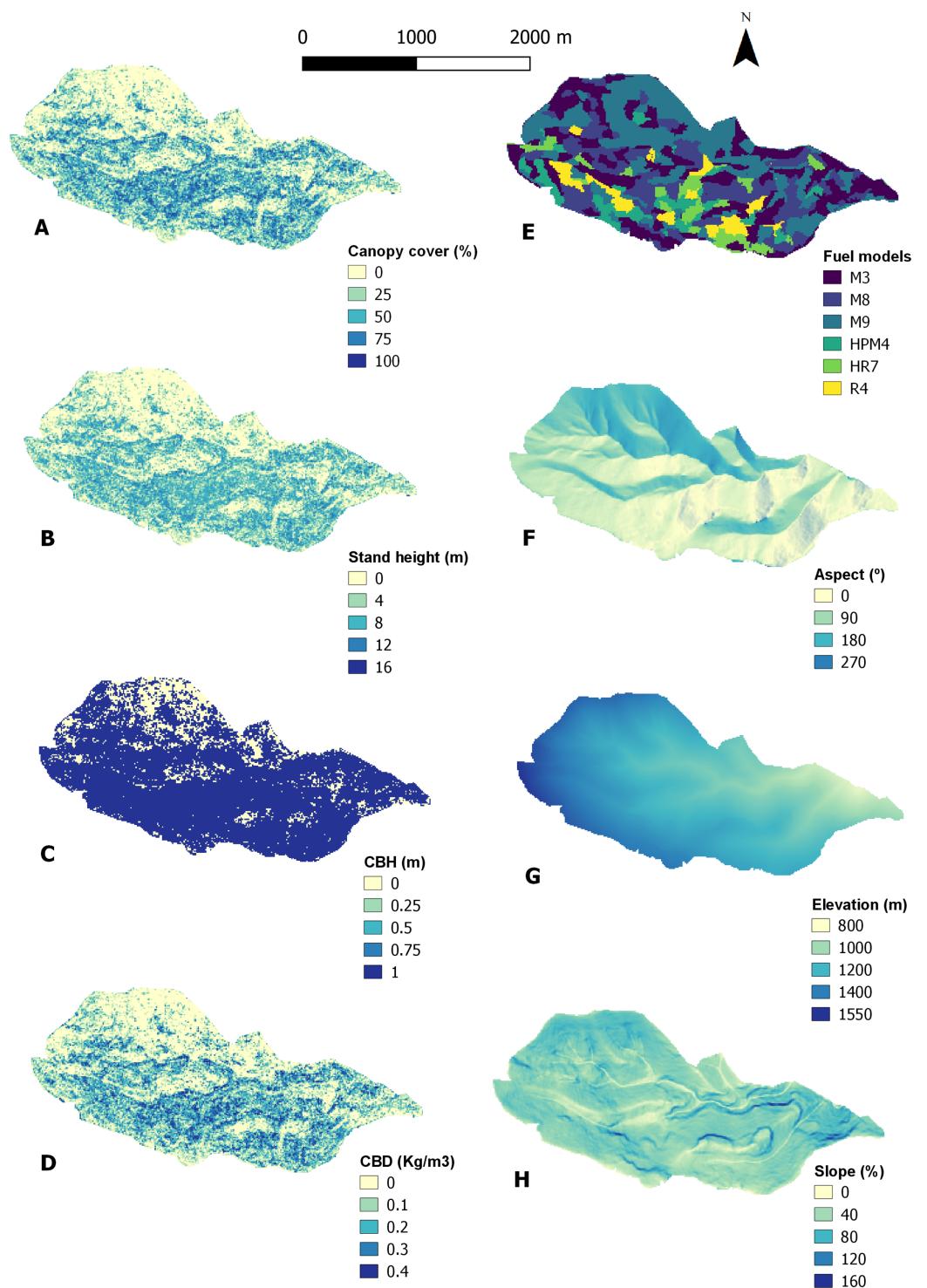
Figure 4 LIDAR raster layers produced to run Flammap. (A) Canopy cover (%). (B) Stand height (m). (C) CBH (m). (D) CBD (Kg/m³). (E) Fuel models. (F) Aspect (°). (G) Elevation (m) (H) Slope (%).
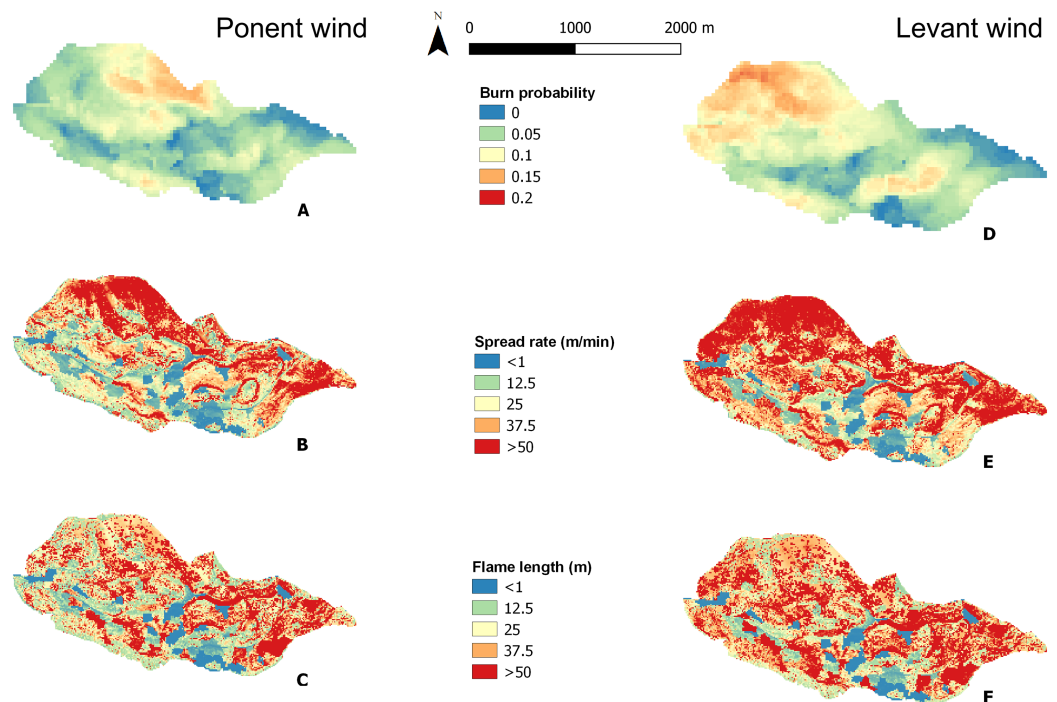
Figure 5 Fire simulations obtained from Flammap for Ponent wind (West) and Levant wind (East) conditions. (A) Burn probability in Ponent wind. (B) Spread rate in Ponent wind (m·min^{-1}). (C) Flame length in Ponent wind (m). (D) Burn probability in Levant wind. (E) Spread rate in Levant wind (m/min). (F) Flame length in Ponent wind (m). Full-size 🖼 DOI: 10.7717/peerj.10158/fig-5
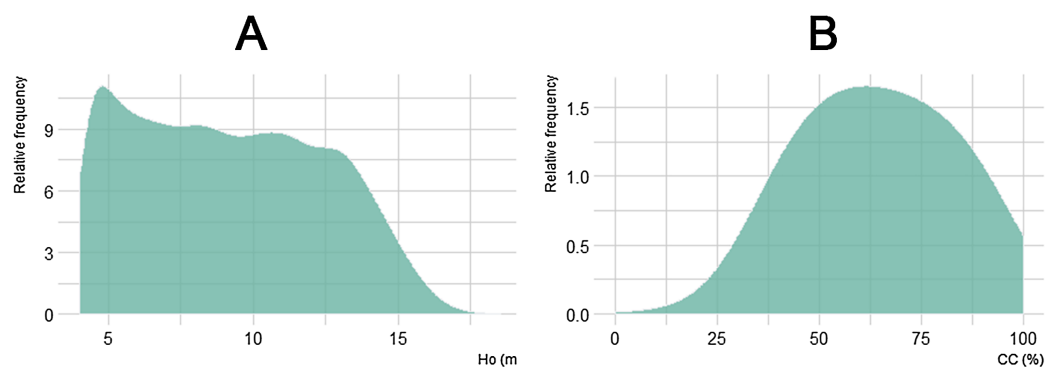
Figure 6 Frequency histograms for canopy height (Ho, A) and canopy cover (CC; B) values, as derived from regressions between Forestereo and LIDAR data, in the studied _A. pinsapo_ forest. Full-size 🖼 DOI: 10.7717/peerj.10158/fig-6

The application of this methodology in the study area obtained fire simulations that showed that east wind conditions ("Levant") resulted in worse fire scenarios than west winds ("Ponent") as illustrated in Fig. 5. Spread rate appears to be more influenced by topography and wind conditions (_Salis et al., 2016_) than by flame length, which appears to be more influenced by fuel characteristics. Low spread rate and flame length were found in areas with HR7 and R4 models because they correspond to high-density _A. pinsapo_ stands, consistent with the findings of _Rodríguez y Silva (1996)_.

Figure 7 Photograph showing the widespread decline and dieback processes (stand stagnation, tree mortality, forest gap opening) that *A. pinsapo* forests are experiencing in the study area. The die-back process of *A. pinsapo* forests stimulates the production of R4 fuel model (abundant dead wood and debris accumulation). Full-size 🖼 DOI: 10.7717/peerj.10158/fig-7

Similar results can be found in the Euro-Mediterranean study of *Salis et al. (2016)*, in which the maximum spread rates simulated in the Attica region (Greece), Budoni (Italy), and Fresnedoso de Ibor and Navalmoral (Spain) are between 50 and 110 m·min^{-1}. In their study, the worst flame length scenarios are located in Fresnedoso de Ibor (Spain) and Penteli (Greece) with a range between 25 and 50 m. They also found a higher spread rate and low flame length mainly in areas with herbaceous vegetation, but also in forest and shrublands in steep mountains exposed to wind (as in our study). In these areas flame length is also higher than in lands with herbaceous vegetation.

However, both wind conditions generate two remarkable foci of fire risk, well highlighted in the burn probability map (Fig. 5). One is in the north-west part of the valley, on south-facing slopes (180° N) where very dense and tall (>1.80 m) patches of the shrub *Juniperus* spp. on steep terrain represent ideal conditions for a high fire spread rate (>50 m·min^{-1}), whereas the flame length will depend more on the wind (Ponent >15 m, Levant >30 m). It is not surprising that this condition corresponds to the M9 fuel model (Table 1), in which massive shrub formations dominate the fire behavior. The other focus is in the eastern part of the valley, due to the occurrence of fuel models for which fire behavior is mainly determined by the combination of dense shrub cover and very steep slopes (>75°).

González-Olabarria et al. (2012) observed a lower fire risk landscape in a carefully managed even-aged forest of *Pinus nigra*. and *P. pinaster*, whereas our study corresponds to a non-managed forest of pinsapo firs. This contrast strengthens the argument for the urgent need for adaptive management of these endemic fir forests, abandoning the traditional paradigm of non-management in biological conservation. The kind of prevailing fuel model appears to be determinant for the fire scenarios obtained, and the current "don't touch" management strategy, together with the invasion by shrubs into forest mortality gaps, seem to promote high fire risk fuel models in the area.

The distribution of canopy structure features depicted in Fig. 6 highlights: (i) that the most frequent stand height barely reaches 5 m, the mean value is just 9.1 m and figures higher than 12–15 m are rare despite the fact that *A. pinsapo* can reach up to 30–35 m in height (*López-Quintanilla et al., 2013*); (ii) that canopy cover has an average value of 64.5%, well below the full-cover criterion under a "set aside" and "no management" strategy since the late 1960s, and patches with 90–100% cover account for less than 10% of the whole area; and (iii) that there is an overall very high variability for both stand height and canopy cover values across the landscape, with a relatively high evenness in both variable distributions, especially regarding tree height. All these results indicate a lack of old-growth stands in the study area, and the predominance of secondary forests, which is consistent with previous studies based on field surveys (*Linares, Carreira & Ochoa, 2011*; *Linares et al., 2013*).

We found considerably high values of canopy density (CBD: Fig. 4), which can increase the risk of severe crown fires (*Arellano Pérez et al., 2017*). These canopy density values in a well below full-cover area, together with low Ho suggests two possible explanations: (i) the high CBD values correspond to full-cover patches with older stands where gaps are still not open and/or (ii) shrub strata are increasing their height above 4 m, interlocking with the canopy. Both are compatible with different phases of forest decline and the gap opening process.

The low stand height values we found, even in the patches with older stands and high cover values, could indicate symptoms of stand stagnation in such patches. A multi-temporal comparison (1957–2007) and fractal analysis of digital panchromatic aerial photographs of the same area (*Linares et al., 2006*; *Linares, Camarero & Carreira, 2009*), revealed a process of simultaneous stand densification and expansion of *A. pinsapo* at the landscape level in the last decades. This is a consequence of strict protection since the 1960s of an area mostly covered at the time by bare soils and open scrublands, with a few sparsely distributed and small stands and isolated trees of *A. pinsapo*. Increasing competition due to the densification of these regenerating even-aged stands led to stand stagnation in the 1980s, which acted as a predisposing factor for the climate change-induced forest decline symptoms reported since 1994–1995, associated with a series of very intense drought spells that acted as an inciting factor (*Linares & Carreira, 2009*). Finally, tree growth decline and loss of vigor led to the expansion of the root-rot fungus pathogen *Heterobasidion abietinum* (*Linares et al., 2010*), which acted as a contributing factor (*Manion, 1981*) causing widespread mortality and extensive formation of forest-gaps in the last two decades (>1/3 of the previous basal area lost).

This multifactorial forest decline and dieback process increases the production of HR7 and R4 fuel models, as shown in Fig. 7. Under the prevalent "no-management" policy, these new open areas are, eventually, being invaded by dense shrubs, as supported by our LIDAR and ForeStereo data. This increases their importance in the fire behavior and promotes fuel models with high fire spread rate such as the UCO M9 fuel type. The fuel model classification revealed a remarkable contribution of M9 (Fig. 4), covering 30.5% of the study area. This suggests that shrub invasion is taking place and is already in an advanced phase. Also, the CBD values point to a high exposure to crown fires (*Arellano Pérez et al., 2017*) and could explain the forecasted high flame length in some areas.

As explained in the Introduction section, fire intensity in pinsapo forests is known to be low, but the above-mentioned current invasion into the mortality gaps by the surrounding dense shrubs could invert this tendency. However, it must be highlighted that the efficacy of employing fire simulations in risk management strongly depends on input data of high accuracy and precision, due to the complex heterogeneity of forest landscapes (*Rodríguez y Silva & Molina-Martínez, 2012*). Although we precisely determined shrub composition and structure in a set of training field plots, the low LIDAR point cloud density available hindered reliable mapping of understory vegetation, which thus may restrict the accuracy of the obtained fire risk simulations. The combined use of LIDAR, both terrestrial and airborne, could be the best option to map fuel models and canopy data such as Canopy Base Height and Canopy Bulk Density, for increased accuracy. Nevertheless, ForeStereo was shown to be a useful alternative to terrestrial LIDAR for calculating stand structure. Our study attempts to set a precedent as the first approach to fire risk analysis in *Abies pinsapo* forests using LIDAR. Also, it demonstrates the significant potential of this method for study of the ecological structure of populations of endangered fir species, and to broaden the understanding of their conservation status. Most of the current work with LIDAR data focuses on forests with commercial interest, and few studies have employed this technology to understand the structure of the populations of endangered species forests and their vulnerability to fire risk.

CONCLUSIONS

Our results show a high fire risk for the largest remaining continuous forest of the relict and endangered *A. pinsapo* tree species. Such risk, especially under east wind conditions (Levant), was found to be associated with a remarkable presence of shrub-dominated fuel models (M9). Using aerial LIDAR and ForeStereo data to assess stand structure spatial variability in the area, we found symptoms of stand stagnation and forest decline under the current no-management conservation policy. This process together with climate change trends triggers the formation of mortality-gaps that are eventually invaded by shrubs, increasing the production of the M9 fuel model, which in turn worsen fire risk. These findings stress the need for proactive adaptive management of *A. pinsapo* forests, including: (i) the creation of bare patches through shrub clearing, (ii) a reinforcement of the firewalls in the west part of the valley and (iii) promotion of grazing and trampling

levels by wild ungulates (or domestic livestock if they were insufficient) to reduce shrub fuel load without compromising *A. pinsapo*. We also support the efficacy of thinning treatments for canopy structural diversity enhancement as an essential tool to avoid stand stagnation (*Linares, Camarero & Carreira, 2009*; *Linares et al., 2009*; *Lechuga et al., 2017*, *2019*) and high CBD values, to reduce the probability of crown fires and thus increase resilience to wildfires (*Koontz et al., 2020*), as well as to reduce climate change-induced tree mortality (*Linares, Camarero & Carreira, 2009*).

The importance of the *A.pinsapo* populations in Sierra de las Nieves is one of the main reasons that inspired Spanish national policy to upgrade this protected area into a National Park. Although the models obtained have low accuracy due to technical limitations, our study provides a preliminary estimate, a first step to assess pinsapo forest risk factors using remote and proximal sensing as essential tools to support conservation management. These methods can also be extended to the monitoring of other endangered Western Mediterranean relict fir forests such as those of *A. numidica* and *A. pinsapo marocana* in North Africa and can be implemented in their conservation strategies.

ABBREVIATIONS

CC	Canopy Cover
CBD	Canopy Bulk Density
CBH	Canopy Base Height
G	Basal area
Ho	Stand height
KIA	Kappa Index of Agreement
MMT	Minimum Travel Time
RMSE	Root-mean-square error
SD	Standard Deviation

ACKNOWLEDGEMENTS

ADDITIONAL INFORMATION AND DECLARATIONS

Funding

Competing Interests

Antonio Flores-Moya is a PeerJ Academic Editor.

Author Contributions

- Álvaro Cortés-Molino conceived and designed the experiments, performed the experiments, analyzed the data, prepared figures and/or tables, authored or reviewed drafts of the paper, and approved the final draft.
- Isabel Aulló-Maestro conceived and designed the experiments, analyzed the data, authored or reviewed drafts of the paper, and approved the final draft.
- Ismael Fernandez-Luque analyzed the data, prepared figures and/or tables, and approved the final draft.
- Antonio Flores-Moya analyzed the data, authored or reviewed drafts of the paper, and approved the final draft.
- José A. Carreira conceived and designed the experiments, performed the experiments, analyzed the data, authored or reviewed drafts of the paper, and approved the final draft.
- A Enrique Salvo analyzed the data, authored or reviewed drafts of the paper, and approved the final draft.

Field Study Permissions

The following information was supplied relating to field study approvals (i.e., approving body and any reference numbers):

Field experiments were approved by the "Consejería de Medio Ambiente y Ordenación del Territorio, Junta de Andalucía". This is the Department of Environment and Land Management from the Andalusian Regional Government (Project number: PNSN/AU/10-2018).

Patent Disclosures

The following patent dependencies were disclosed by the authors:

ForeStereo, based on MU2005-01738, patented by INIA-CIFOR in 2005

Patent disclosure: http://consultas2.oepm.es/InvenesWeb/detalle?p=1&referencia=U200501738.

Data Availability

The following information was supplied regarding data availability:

Raw data are available as a Supplemental File.

Supplemental Information

Supplemental information for this article can be found online at http://dx.doi.org/10.7717/peerj.10158#supplemental-information.

REFERENCES

Adamic M, Diaci J, Rozman A, Hladnik D. 2017. Long-term use of uneven-aged silviculture in mixed mountain Dinaric forests: a comparison of old-growth and managed stands. *Forestry* **90(2)**:279–291 DOI 10.1093/forestry/cpw052.

Ahmed OS, Franklin SE, Wulder MA, White JC. 2015. Characterizing stand-level forest canopy cover and height using Landsat time series, samples of airborne LIDAR, and the random forest

algorithm. *ISPRS Journal of Photogrammetry and Remote Sensing* **101**:89–101
DOI 10.1016/j.isprsjprs.2014.11.007.

Alcasena FJ, Ager AA, Bailey JD, Pineda N, Vega-García C. 2019. Towards a comprehensive wildfire management strategy for Mediterranean areas: framework development and implementation in Catalonia. *Spain Journal of Environmental Management* **231**:303–320
DOI 10.1016/j.jenvman.2018.10.027.

Anderson HE. 1982. Aids to determining fuel models for estimating fire behavior. *General Technical Report INT-122*, United States Department of Agriculture, Forest Service, Intermountain Forest and Range Experiment Station, Ogden, UT, 26.

Aragón JF, Navarro Cerrillo R, Mesas Carrascosa F. 2019. Validación de un paratrike como plataforma para la captación de imágenes de alta resolución en formaciones de Abies pinsapo Boiss. *Cuadernos de la Sociedad Española de Ciencias Forestales* **45(2)**:171–204
DOI 10.31167/csecfv5i45.19875.

Arellano Pérez S, González Álvarez JG, Vega Hidalgo JA, Ruiz González AD. 2017. *Modelos de estimación de la distribución vertical de combustibles finos de copas en masas de pinar a partir de datos del IV Inventario Forestal Nacional.* Plasencia: 7° Congreso Forestal Español.

Arumäe T, Lang M. 2018. Estimation of canopy cover in dense mixed-species forests using airborne lidar data. *European Journal of Remote Sensing* **51(1)**:132–141
DOI 10.1080/22797254.2017.1411169.

Asensi A, Rivas-Martínez S. 1976. Contribución al conocimiento fitosociológico de los pinsapares de la Serranía de Ronda. *Anales Instituto Botánico Cavanilles* **33**:239–247.

Assman E. 1970. *The principles of forest yield study.* Oxford: Pergamon Press, 506.

Botequim B, Fernandes PM, Borges JG, González-Ferreiro E, Guerra-Hernández J. 2019. Improving silvicultural practices for Mediterranean forests through fire behavior modeling using LiDAR-derived canopy fuel characteristics. *International Journal of Wildland Fire* **28(11)**:823–839 DOI 10.1071/WF19001.

Bowman D, Balch JK, Artaxa P, Bond WJ, Carlson JM, Cochrane MA, D'Antonio CS, DeFries R. 2009. Fire in the Earth System. *Science* **324(5926)**:481–484
DOI 10.1126/science.1163886.

Chianucci F. 2019. An overview of in situ digital photographic approaches to estimate forest canopy attributes. *Canadian Journal of Forest Research* **76(3)**:227–242
DOI 10.1139/cjfr-2019-0055.

Chuvieco E, Riaño D, Danson FM, Martin P. 2006. Use of a radiative transfer model to simulate the postfire spectral response to burn severity. *Journal of Geophysical Research: Biogeosciences* **111(G4)**:3683 DOI 10.1029/2005JG000143.

Chuvieco E, Kasischke ES. 2007. Remote sensing information for fire management and fire effects assessment. *Journal of Geophysical Research: Biogeosciences* **112(G1)**:9
DOI 10.1029/2006JG000230.

Cortés-Molino A, Melero Jiménez IJ, Fernández Luque I, Flores-Moya A, Salvo Tierra AE. 2017. *Análisis de la estructura de la vegetación del poljé de la Nava de los Pinsapos mediante tecnología LIDAR.* Murcia: Asociación Española de Teledetección.

De Sousa CH, Hilker T, Waring R, De Moura YM, Lyapustin A. 2017. Progress in remote sensing of photosynthetic activity over the Amazon Basin. *Remote Sensing* **9(1)**:48
DOI 10.3390/rs9010048.

Dzikiti S, Jovanovic NZ, Bugan RD, Majozi NP, Nickless A, Cho MA, Le Maitre DC, Ntshidi Z, Pienaar HH. 2019. Comparison of two remote sensing models for estimating

evapotranspiration: algorithm evaluation and application in seasonally arid ecosystems in South Africa. *Journal of Arid Land* **11(4)**:495–512 DOI 10.1007/s40333-019-0098-2.

Finney M. 2002. Fire growth using minimum travel time methods. *Canadian Journal of Forest Research* **32(8)**:1420–1424 DOI 10.1139/x02-068.

Finney MA. 2006. An overview of FlamMap fire modeling capabilities. *USDA Forest Service Proceedings* **41**:213–220.

Furyaev V, Wein WR, MacLean DA. 1983. Fire influences in Abies-dominated forests. In: MacLean RW, ed. *The role of fire in Northern Circumpolar Ecosystems.* Chinchester: John Wiley & Sons, 221–234.

Gao Y, Mas JM, Niemeyer I, Marpu PR, Palacio JL. 2007. *Object-based image analysis for mapping land-cover in a forest area.* Enschede: International Symposium for Spatial Date Quality (ISSDQ).

González-Olabarria JR, Rodríguez F, Fernández-Landa A, Yudego-Mola B. 2012. Mapping fire risk in the Model Forest of Urbión (Spain) based on airborne LIDAR measurements. *Forest Ecology and Management* **282**:149–156 DOI 10.1016/j.foreco.2012.06.056.

Hall RJ, Fournier AF, Rich P. 2017. Introduction. In: Fournier RA, Hall RJ, eds. *Hemispherical Photography in Forest Science: Theory, Methods, and Applications.* Vol. 28. Springer Netherlands, 313.

He T, Pausas JG, Belcher CM, Schwilk DW, Lamont BB. 2012. Fire adapted traits of Pinus arose in the fiery Cretaceous. *New Phytologist* **194(3)**:751–759 DOI 10.1111/j.1469-8137.2012.04079.x.

Hilker T, Coops NC, Newnham GJ, Van Leeuwen M, Wulder MA, Stewart J, Culvenor DS. 2012. Comparison of terrestrial and airborne LIDAR in describing stand structure of a thinned lodgepole pine forest. *Journal of Forestry* **110(2)**:97–104 DOI 10.5849/jof.11-003.

Immitzer M, Atzberger C. 2014. Early detection of bark beetle infestation in Norway Spruce (*Picea Abies*, L.) using WorldView-2 Data. *Photogrammetrie - Fernerkundung - Geoinformation* **2014(5)**:351–367 DOI 10.1127/1432-8364/2014/0229.

Koontz MJ, North MP, Werner CM, Fick SE, Latimer AM. 2020. Local forest structure variability increases resilience to wildfire in dry western U.S. coniferous forests. *Ecology Letters* **23**:483–494 DOI 10.1111/ele.13447.

Lechuga V, Carraro V, Viñegla B, Carreira JA, Linares JC. 2017. Managing drought-sensitive forests under global change. low competition enhances long-term growth and water uptake in Abies pinsapo. *Forest Ecology and Management* **406**:72–82 DOI 10.1016/j.foreco.2017.10.017.

Lechuga V, Carraro V, Viñegla B, Carreira JA, Linares JC. 2019. Carbon limitation and drought sensitivity at contrasting elevation and competition of Abies pinsapo forests: does experimental thinning enhance water supply and carbohydrates? *Forests* **10(12)**:1132 DOI 10.3390/f10121132.

Liepelt S, Mayland-Quellhorst E, Lahme M, Ziegenhagen B. 2010. Contrasting geographical patterns of ancient and modern genetic lineages in Mediterranean Abies species. *Plant Systematics and Evolution* **284(3–4)**:141–151 DOI 10.1007/s00606-009-0247-8.

Linares JC, Esteban FJ, Viñegla B, Carreira JA. 2006. A computational analysis of multi-temporal vegetation changes using the fractal dimension spectrum. *Harmonic and Fractal Image Analysis* **1**:97–100.

Linares JC. 2008. Effects of global change overpopulation dynamic and ecophysiology of Abies pinsapo Boiss relictian forests. Ph.D. thesis, University of Jaén.

Linares JC, Camarero JJ, Carreira JA. 2009. Interacting effects of changes in climate and forest cover on mortality and growth of the southernmost European fir forests. *Global Ecology and Biogeography* **18(4)**:485–497 DOI 10.1111/j.1466-8238.2009.00465.x.

Linares JC, Carreira JA. 2009. Temperate-like stand dynamics in relict Mediterranean-fir (Abies pinsapo, Boiss.) forests from southern Spain. *Annals of Forest Sciences* **66(6)**:610 DOI 10.1051/forest/2009040.

Linares JC, Camarero JJ, Carreira JA. 2009. Plastics responses of Abies pinsapo xylogenesis to drought and competition. *Tree Physiology* **29(12)**:1525–1536 DOI 10.1093/treephys/tpp084.

Linares J-C, Delgado-Huertas A, Julio Camarero J, Merino J, Carreira JA. 2009. Competition and drought limit the response of water-use efficiency to rising atmospheric carbon dioxide in the Mediterranean fir Abies pinsapo. *Global Change Ecology* **161(3)**:611–624 DOI 10.1007/s00442-009-1409-7.

Linares JC, Camarero JJ, Bowker MA, Ochoa V, Carreira JA. 2010. Stand-structural effects on Heterobasidion abietinum-related mortality following drought events in Abies pinsapo. *Global Change Ecology* **164(4)**:1107–11019 DOI 10.1007/s00442-010-1770-6.

Linares JC. 2011. Biogeography and evolution of *Abies* (*Pinaceae*) in the Mediterranean Basin: the roles of long-term climatic changes and glacial refugia. *Journal of Biogeography* **38(4)**:619–630 DOI 10.1111/j.1365-2699.2010.02458.x.

Linares JC, Carreira JA, Ochoa V. 2011. Human impacts drive forest structure and diversity: insights from Mediterranean mountain forest dominated by Abies pinsapo (Boiss.). *European Journal of Forest Research* **130(4)**:533–542 DOI 10.1007/s10342-010-0441-9.

Linares JC, Delgado-Huertas A, Carreira JA. 2011. Climatic trends and different drought adaptive capacity and vulnerability in a mixed Abies pinsapo- Pinus halepensis forest. *Climate Change* **105(1–2)**:67–90 DOI 10.1007/s10584-010-9878-6.

Linares JC, Camarero JJ, Delgado-Huertas A, Carreira JA, López-Quintanilla J, Navarro RM, Carreira JA, Coca M, Rodríguez C. 2013. Capítulo 24: Efectos de los cambios de clima y usos del territorio sobre la dinámica y el crecimiento de los bosques de *Abies pinsapo* en las últimas décadas. In: López-Quintanilla J, Navarro RM, Carreira JA, Coca M, Rodríguez C, eds. *Los pinsapares (Abies pinsapo Boiss.) en Andalucía: Conservación y sostenibilidad en el siglo XX1.* Vol. 24. Córdoba: Junta de Andalucía y Universidad de Córdoba, 401–412.

López-Quintanilla J, Navarro RM, Carreira JA, Coca M, Rodríguez C. 2013. *Los pinsapares (Abies pinsapo Boiss.) en Andalucía: Conservación y sostenibilidad en el siglo XXI.* Córdoba: Junta de Andalucía y Universidad de Córdoba, 576.

Mallinis G, Mitsopoulos I, Beltran E, Goldamer JG. 2016. Assessing wildfire risk in cultural heritage properties using high spatial and temporal resolution satellite imagery and spatially explicit fire simulations: the case of Holy Mount Athos. *Greece Forests* **7(2)**:46 DOI 10.3390/f7020046.

Manion P. 1981. *Tree disease concepts.* Englewood Cliffs: Prentice-Hall.

Marino E, Montesa F, Tomé JL, Navarro JA, Hernando C. 2018. Vertical forest structure analysis for wildfire prevention: comparing airborne laser scanning data and stereoscopic hemispherical images. *International Journal of Applied Earth Observation and Geoinformation* **73**:438–449 DOI 10.1016/j.jag.2018.07.015.

McGaughey RJ, Carson WW. 2003. Fusing LIDAR data, photographs and other data using 2D, and 3D visualization techniques. In: *Proceedings of Terrain Data: Applications and Visualization-Making the Connection.* 16–24.

Mitsopoulos I, Mallinis G, Arianoutsu M. 2015. Wildfire risk assessment in a typical Mediterranean wildland-urban interface of Greece. *Environmental Management* **55(4)**:900–915 DOI 10.1007/s00267-014-0432-6.

Molina JR, Rodríguez y Silva F, Herrera MA. 2017. Economic vulnerability of fire-prone landscapes in protected natural areas: application in a Mediterranean Natural Park. *European Journal of Forest Research* **136(4)**:609–624 DOI 10.1007/s10342-017-1059-y.

Montes F, Rubio-Cuadrado Á, Sánchez-González M, Aulló-Maestro I, Cabrera M, Gómez C. 2019. Occlusion probability in operational forest inventory field sampling with ForeStereo. *Photogrammetric Engineering and Remote Sensing* **85(7)**:493–508 DOI 10.14358/PERS.85.7.493.

Mura M, McRoberts RE, Chirice G, Marchetti M. 2015. Estimating and mapping forest structural diversity using airborne laser scanning data. *Remote Sensing of Environment* **170**:133–142 DOI 10.1016/j.rse.2015.09.016.

Narváez D. 1991. *Extinguido el incendio que ha arrasado 9.000 hectáreas en la Serranía de Ronda*. Madrid: El País.

Pasta S, Sala G, La Mantia T, Bondi C, Tinner W. 2019. The past distribution *of Abies nebrodensis* (Lojac.) Mattei: results of a multidisciplinary study. *Vegetation History and Archaeobotany* **29(3)**:357–371 DOI 10.1007/s00334-019-00747-0.

Pausas JG, Keeley JE. 2009. A burning story: the role of fire in the history of life. *BioScience* **59(7)**:593–601 DOI 10.1525/bio.2009.59.7.10.

Rivas-Martínez S, Rivas-Sáenz S. 1996. *Worldwide bioclimatic classification system*. Spain: Phytosociological Research Center. *Available at* http://www.globalbioclimatics.org.

Rodríguez y Silva F. 1996. Protección y defensa de los pinsapares ante los incendios forestales. In: *Jornadas técnicas internacionales sobre recuperación de pinsapares, 12–14 December, Grazalema.*

Rodríguez y Silva F, Molina Martínez JR. 2010. *Manual técnico para la modelización de la combustibilidad asociada a los ecosistemas forestales mediterráneos*. Córdoba: Forest Fire Lab Defence, University of Córdoba.

Rodríguez y Silva F, Molina-Martínez J. 2012. Modeling Mediterranean forest fuels by integrating field data and mapping tools. *European Journal of Forest Research* **131(3)**:571–582 DOI 10.1007/s10342-011-0532-2.

Rodríguez-García C, Montes F, Ruiz F, Cañellas I, Pita P. 2014. Stem mapping and estimating standing volume from stereoscopic hemispherical images. *European Journal of Forest Research* **133(5)**:895–904 DOI 10.1007/s10342-014-0806-6.

Ruiz-Peinado R, Del Río M, Montero G. 2011. New models for estimating the carbon sink capacity of Spanish softwood species. *Forest Systems* **I(20)**:176–188 DOI 10.5424/fs/2011201-11643.

Rundel PW. 2019. A neogene heritage: conifer distributions and endemism in mediterranean-climate ecosystems. *Frontiers in Ecology and Evolution* **7**:160 DOI 10.3389/fevo.2019.00364.

Salis M, Ager AA, Alcasena FJ, Arca B, Finney MA, Pellizzaro G, Spano D. 2015. Analyzing seasonal patterns of wildfire exposure factors in Sardinia. *Italy Environmental Monitoring and Assessment* **187(1)**:4175 DOI 10.1007/s10661-014-4175-x.

Salis M, Arca B, Alcasena F, Arianoutsou M, Bacciu V, Duce P, Duguy B, Koutsias N, Mallinis G, Mitsopoulos I, Moreno JM, Pérez JR, Urbieta IR, Xystrakis F, Zavala G, Spano D. 2016. Predicting wildfire spread and behavior in Mediterranean landscapes. *International Journal of Wildland Fire* **25**:1015–1032 DOI 10.1071/WF15081.

Sánchez-González M, Cabrera M, Herrera PJ, Vallejo R, Cañellas I, Montes F. 2016. Basal area and diameter distribution estimation using stereoscopic hemispherical images. *Photogrammetric Engineering & Remote sensing* **82**:605–616 DOI 10.14358/PERS.82.8.605.

Sánchez-Salguero R, Camarero JJ, Carrer M, Gutiérrez EA, Andreu-Hayles L, Hevia A, Koutavas A, Martínez-Sancho E, Nola P, Papadopulos A, Pasho E, Toromani E, Carreira JA, Linares JC. 2017. Climate extremes and predicted warming threaten Mediterranean Holocene firs forests refugia. *Proceedings of National Academy of Sciences* **114(47)**:E10142–E10150 DOI 10.1073/pnas.1708109114.

Scott JH, Burgan RE. 2005. *Standard fire behavior fuel models: a comprehensive set for use with Rothermel's surface fire spread model.* Fort Collins: U.S. Department of Agriculture, Forest Service, Rocky Mountain Research Station, 72.

Van Ardt JA, Wynne R, Scrivani J. 2008. Lidar-based mapping of forest volume and biomass by taxonomic group using structurally homogenous segments. *Photogrammetric Engineering and Remote Sensing* **75(8)**:1033–1044 DOI 10.14358/PERS.74.8.1033.

Vega Hidalgo JA. 1999. *Historia del fuego de Pinus pinaster y Abies pinsapo en la carta norte de Sierra Bermeja (Málaga): 1817–1997. Incendios históricos, una aproximación multidisciplinar.* Baeza: UNIA.

Wang C, Glenn NF. 2008. A linear regression method for tree canopy height estimation using airborne lidar data. *Canadian Journal of Remote Sensing* **34(Suppl. 2)**:S217–S227 DOI 10.5589/m08-043.

Wang Z, Ginzler C, Waser LT. 2020. Assessing structural changes at the forest edge using kernel density estimation. *Forest Ecology and Management* **456**:117639 DOI 10.1016/j.foreco.2019.117639.

Wüest RO, Bergamini A, Bollmann K, Baltensweiler A. 2020. LiDAR data as a proxy for light availability improve distribution modeling of woody species. *Forest Ecology and Management* **456**:117644 DOI 10.1016/j.foreco.2019.117644.

Yebra M, Quan X, Riaño D, Rozas Larraondo P, Van Dijk AIJM, Cary GJ. 2018. A fuel moisture content and flammability monitoring methodology for continental Australia based on optical remote sensing. *Remote Sensing of Environment* **212**:260–272 DOI 10.1016/j.rse.2018.04.053.